

Ballooning Mode Stability of Bean-Shaped Cross Sections for High- β Tokamak Plasmas

M. S. Chance, S. C. Jardin, and T. H. Stix

Plasma Physics Laboratory, Princeton University, Princeton, New Jersey 08544

(Received 16 August 1983)

Indentation of a tokamak plasma on its inner-major-radius side is shown to be strongly beneficial for achieving high- β stability against ballooning modes. With use of a set of reasonable equilibrium profiles, it is found that moderate indentation provides accessibility to the second region of stability. Ohmic equilibrium configurations which exhibit the second stability region have not yet been found.

PACS numbers: 52.55.Gb, 52.30.+r, 52.35.Py, 52.65.+z

The capability to create and maintain stable plasmas with $\beta \geq 20\%$ would comprise a major technological advantage for a tokamak reactor. However, the magnetohydrodynamic (MHD) ballooning instability could be a serious obstacle to this goal. Several studies have been carried out to find environments favorable for suppressing this mode.^{1,2} Recently, an empirical shape-optimization study by Miller and Moore³ has shown that a bean-shaped plasma—inwardly concave at the inner-major-radius side—can enhance the achievable stable β against ballooning. A similar shape had earlier been found by Mercier⁴ to enhance stability against localized interchange. In this paper we find that bean shapes can exhibit strong local magnetic shear and short connection lengths and, in fact, under certain modest conditions make accessible the second region of stability against ballooning modes.

If we write $\vec{B} = \nabla\varphi \times \nabla\psi + g\nabla\varphi \equiv \nabla\alpha \times \nabla\psi$, $\vec{J} \times \vec{B} = \nabla p$, and $\nabla \times \vec{B} = \vec{J}$, the Grad-Shafranov equation takes the form

$$\nabla \cdot x^{-2} \nabla \psi = \vec{J} \cdot \nabla \varphi = -(p' + gg'/x^2). \quad (1)$$

The poloidal flux is $2\pi\psi$, x is the major radius, φ is the azimuthal angle in the cylindrical coordinates (x, φ, z) , and primes denote differentiation with respect to ψ . Equation (1) is solved by use of a flux coordinate code⁵ in the fixed-boundary mode, specifying the shape of the plasma boundary. This shape is given by the "bean" equation,

$$x = \bar{x} + \rho \cos\gamma, \quad z = E\rho \sin\gamma, \quad (2)$$

where $\rho = A(1 + B \cos t)$, $\gamma = C \sin t$, and $0 \leq t < 2\pi$ so that $-C \leq \gamma < C$. Given A , B , C , and E , the aspect ratio is fixed by the choice of \bar{x} . Unless otherwise stated, $A = 1.0$, $B = 0.6$, $b/a = 1.386$, and $R/a = 4.0$ (Fig. 1). The indentation parameter, $d/2a$, is adjusted by changing C .

It is apparent even looking casually at the magnetic surfaces that a line of force on an outer bean surface spends most of its life at values of

major radius smaller than the magnetic-axis major radius. Because $dl \sim R d\varphi$ and $B \sim 1/R$, bean shaping can easily make $u = \oint dl/B$ smaller on the outer surfaces than on the magnetic axis. Together with finite shear, this average magnetic well tends to stabilize interchange modes. Nevertheless, the plasma may be susceptible to ballooning perturbations which adjust themselves within a surface to be large where the well is weak or nonexistent, and small otherwise. These modes are described by the ballooning equation which can be written in the form⁶⁻⁸

$$\begin{aligned} \vec{B} \cdot \nabla \left[\left(\frac{1}{|\nabla\psi|^2} + \frac{|\nabla\psi|^2}{B^2} I^2 \right) \vec{B} \cdot \nabla \Phi \right] \\ + \frac{2p'}{B^2} \left[\frac{B^2}{|\nabla\psi|^2} \kappa_\psi - I \kappa_s \right] \Phi \\ + \rho \omega^2 \left(\frac{1}{|\nabla\psi|^2} + \frac{|\nabla\psi|^2}{B^2} I^2 \right) \Phi = 0, \quad (3) \end{aligned}$$

where $\kappa_\psi = \vec{k} \cdot \nabla\psi$, $\kappa_s = \vec{k} \cdot \vec{B} \times \nabla\psi$, and $\vec{k} = (\vec{B}/B) \cdot (\nabla\vec{B}/B)$. The first term contains the effect of field tension, the second contains the potentially

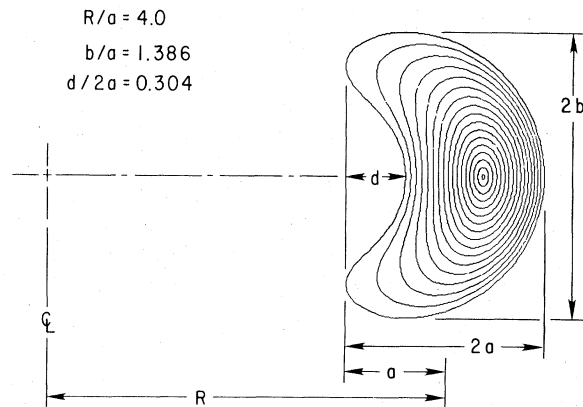


FIG. 1. Geometry used to calculate the fixed-boundary equilibria. The flux surfaces are spaced in equal increments of $\psi^{1/2}$.

destabilizing pressure-curvature combination, and the third term stems from fluid inertia.

Both the connection length and the local magnetic shear, S , play important roles in ballooning stability theory.⁸ The dependence of Eq. (3) on S occurs through the integrated local shear, I ; we have

$$\begin{aligned} S &= -\frac{\vec{B} \times \nabla \psi}{|\nabla \psi|^2} \cdot \nabla \times \frac{\vec{B} \times \nabla \psi}{|\nabla \psi|^2} \\ &= -\vec{B} \cdot \nabla \left(\frac{\nabla \alpha \cdot \nabla \psi}{|\nabla \psi|^2} \right) \equiv \vec{B} \cdot \nabla I \\ &= \frac{1}{g} \left[\left(\frac{g g'}{x^2} \right)' + \frac{\partial}{\partial \theta} \left(\frac{\nabla \psi \cdot \nabla \theta}{|\nabla \psi|^2} \frac{g g'}{x^2} \right) \right], \end{aligned} \quad (4)$$

where

$$g \equiv (\nabla \psi \times \nabla \theta \cdot \nabla \varphi)^{-1}.$$

Since $q(\psi) = (1/2\pi) \oint g g' / x^2 d\theta$, then $(1/2\pi) \oint S g d\theta = q'(\psi)$, so that S is comprised of the averaged global shear $q'(\psi)$ plus a residual oscillating part.

In a conventional tokamak the residual contribution to S can be so negative on the outer of the major radius, where the poloidal field is usually the strongest, as to make S vanish there [cf. Fig. 2(a)]. The vanishing of S is the condition that surfaces containing both \vec{B} and $\nabla \psi$ exist and the local interchange of magnetic field lines can be most easily realized on such surfaces. However, a strong outward shift of the magnetic axis can appreciably strengthen the poloidal magnetic field on the outside and cause the vanishing points of S to move away from the destabilizing region. This shift may be realized by increasing the pressure but, unfortunately, the onset of the instability usually occurs before local shear and/or connection length stabilization actually takes place. Another route to stability, exploited here, is to indent the plasma on its inner-major-radius side so that the axis is effectively shifted even at low β . Further increase of the pressure enhances the shift even more, thus rendering the plasma immune to instability.

Contours of constant local shear in the neighborhood of $S=0$ are shown in Fig. 2(a) for a moderately indented low- β plasma. The local shear here is zero and/or weak in the outer region of the plasma. Increasing the pressure at this indentation causes instability at about $\beta \sim 2.6\%$. A stronger indentation, as shown in Fig. 2(b), moves the $S=0$ contour farther out. In this case, even though the shear is still weak at low β [Fig. 2(b)] an increase in pressure [Fig. 2(c)] strengthens the local shear at large major radius, pre-

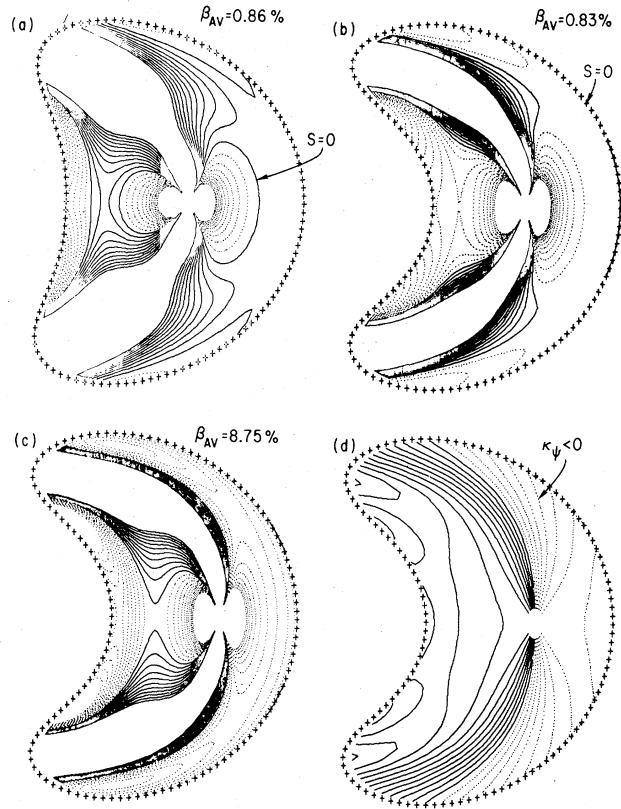


FIG. 2. (a)-(c): Contours of constant local shear S at and near $S=0$ showing its variation with β and indentation. (d) Contours of constant normal magnetic curvature.

serving stability by the self-healing process.⁹

Stabilization due to the shortened connection length of the indented plasma is also effective. The strong poloidal field at the outside of the torus due to the indentation and finite pressure causes the magnetic field lines to move rapidly through the bad-curvature region while lingering at the tips of the bean which are generally located in areas of favorable normal curvature. As seen in Fig. 2(d) there is a clear reduction in the size of the dangerous region, where the normal curvature is negative.

The effect of indentation was first studied by numerical solutions of Eq. (3) with the profiles $q(y) = \sum q_i y^i$, $0 \leq i \leq 3$, and $p(y) = p_0(1-y)^2$, where $y = \psi/\Delta\psi$, $2\pi\Delta\psi$ being the poloidal flux within the plasma. The coefficients q_i were specified such that $q(0) = 1.03$, $q(1) = 4.2$, $q'(0) = 0.84375$, and $q'(1) = 9.0$. The results are shown in Fig. 3. At low indentation it is seen that an increase of $\beta_{av} \equiv 2 \int p dv / \int B^2 dv$ (obtained by increasing p_0) causes the plasma to become balloon unstable,

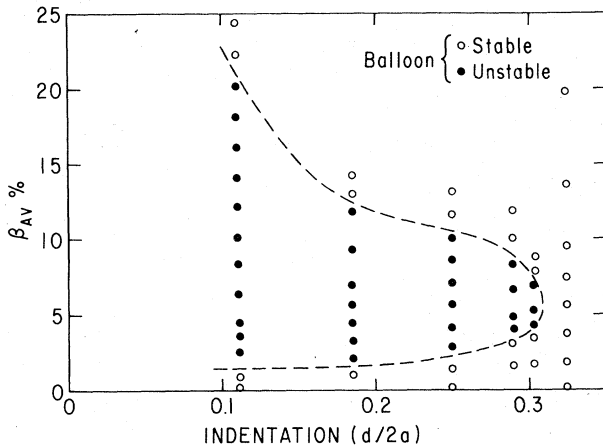


FIG. 3. Stability plot of β vs indentation showing the first and second regions of stability at low indentation. At sufficiently high indentation the second region becomes accessible.

but further increase of the pressure places the plasma in the so-called second stability regime.⁸⁻¹³ Moreover, if the indentation is large enough, increasing the plasma pressure bypasses the unstable region completely. Bean shaping thus provides a path for access to the second region of stability of ballooning modes.

An alternative method for parametrizing the equilibrium, instead of specifying the $q(y)$ and $p(y)$ profiles, is to fix the temperature profile and then to use the Ohmic equilibrium condition, $\langle \vec{J} \cdot \vec{B} \rangle / \langle \vec{B} \cdot \nabla \phi \rangle = K T_e^{3/2}$, to prescribe the current distribution. The free parameter, K , is used to determine either the total plasma current or the safety factor on the magnetic axis. We then use $T_e(\psi) = T_0 [1 - y^4]$ and $p(\psi) = p_0 [1 - y^2]^2$, the latter being the same as in the flux-conserving sequence described previously for the results in Fig. 3. The exponents in the T_e profile were chosen to avoid excessive current peaking and the corresponding large shear or lack of equilibrium. Figure 4 shows $J_{\parallel av}$ for several equilibrium configurations from Fig. 3 corresponding to different β values for the indentation $d/2a = 0.3$. For the prescribed- q equilibrium at low β , the temperature profile is broad, has a plateau near the outer edge, and does not go smoothly to zero, but to a pedestal value $T_e(\text{edge}) \sim \frac{1}{2} T_e(\text{center})$.

This Ohmic equilibrium study is summarized in Fig. 5, showing contours of λ , the infinite- n eigenvalue on the most unstable surface, for a continuous range of q_0 and $\langle \beta \rangle$. These configurations provide improved β values in the first stability regime, but a second regime exhibiting com-

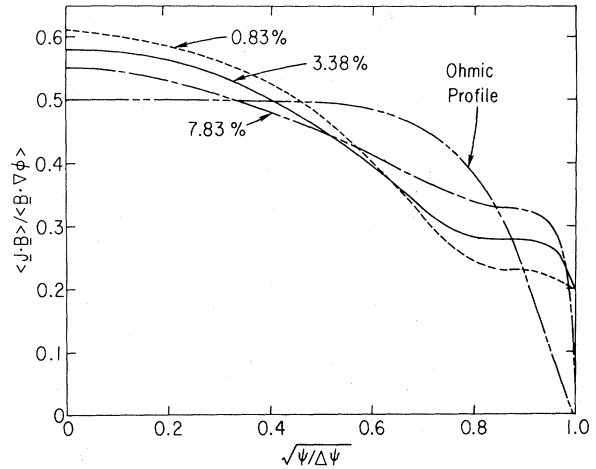


FIG. 4. $J_{\parallel av}$ for equilibria where $q(\psi)$ is prescribed. The double-dashed curve is the corresponding profile used in the Ohmic equilibrium studies where $T_e(\psi)$ is prescribed.

plete stabilization has not been obtained. It appears likely that the second regime may lie in the upper right-hand corner of this diagram, but a competing tendency for q_{edge} to increase as both q_0 and $\langle \beta \rangle$ increase makes obtaining equilibrium difficult in this region. Different temperature profiles may possibly exhibit the second stable regime, and some tailoring of experimental profiles can be effected by adjusting the time signature of the tokamak transformer-induced loop voltage. There are also non-Ohmic supplementary heating methods and a future potential

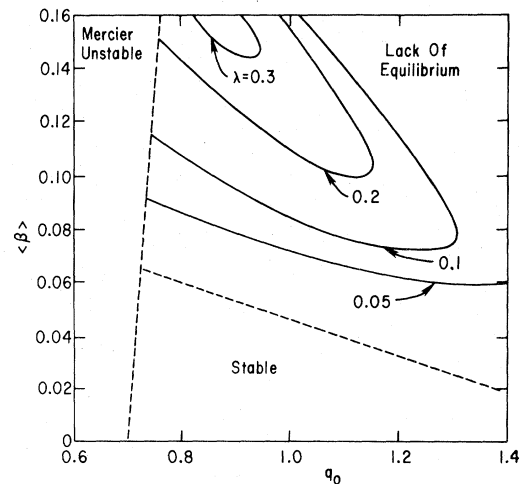


FIG. 5. Stability diagram for ballooning modes when the Ohmic equilibrium condition is used. Here $\lambda = \rho \omega^2$.

for steady-state current drive in which case the current may have significant deviation from the Ohmic one. It should be pointed out that the studies by Mercier¹² on a class of supplementary-heated kidney-shaped configurations resulted in plasmas stable for $\beta \lesssim 3\% - 5\%$.

In future papers we shall discuss stability against low- n MHD modes, finite-Larmor-radius modifications of the ballooning modes, and particle orbit-confinement properties.

Discussions and cooperation with Dr. R. C. Grimm, Dr. D. A. Monticello, Dr. A. H. Boozer, and Dr. F. W. Perkins and other co-workers at Princeton University are greatly appreciated. In addition we are pleased to acknowledge the interest and encouragement of Dr. H. P. Furth and Dr. P. H. Rutherford.

This work was supported by U. S. Department of Energy Contract No. DE-AC02-76-CHO-3073.

¹A. M. Todd, J. Manickam, M. Okabayashi, M. S. Chance, R. C. Grimm, J. M. Greene, and J. L. Johnson, Nucl. Fusion 19, 743 (1979).

²L. C. Bernard, D. Dobrott, F. J. Helton, and R. W. Moore, Nucl. Fusion 20, 1199 (1980).

³R. Miller and R. W. Moore, Phys. Rev. Lett. 43, 765 (1979).

⁴C. Mercier, in *Lectures in Plasma Physics*, EURATOM-CEA/CEN/EUR 5/27e (EURATOM, Luxembourg, 1974).

⁵J. DeLucia, S. C. Jardin, and A. M. M. Todd, J. Comput. Phys. 37, 183 (1980).

⁶D. Dobrott, D. B. Nelson, J. M. Greene, A. H. Glasser, M. S. Chance, and E. A. Frieman, Phys. Rev. Lett. 39, 943 (1977).

⁷J. W. Connor, R. J. Hastie, and J. B. Taylor, Phys. Rev. Lett. 40, 396 (1978).

⁸J. M. Greene and M. S. Chance, Nucl. Fusion 21, 453 (1981).

⁹B. Coppi, A. Ferreira, and J. J. Ramos, Phys. Rev. Lett. 44, 990 (1980).

¹⁰D. Lortz and J. Nührenberg, Phys. Lett. 68A, 49 (1978).

¹¹H. R. Strauss, W. Park, D. A. Monticello, R. B. White, S. C. Jardin, M. S. Chance, A. M. M. Todd, and A. H. Glasser, Nucl. Fusion 20, 638 (1980).

¹²C. Mercier, in *Plasma Physics and Controlled Nuclear Fusion Research* (International Atomic Energy Agency, Vienna, 1979), Vol. 1, p. 701.

¹³L. Sugiyama and J. W.-K. Mark, Phys. Lett. 84A, 123 (1981).